

Temperature Dependence of the Ultrasonic Attenuation in Germanium*

BARRY I. MILLER†

Department of Physics and Institute for the Study of Metals, University of Chicago, Chicago, Illinois

(Received 28 June 1963)

The ultrasonic attenuation in germanium has been measured as a function of temperature from 300 to 20°K and at frequencies of 4 to 132 Mc/sec. The measurements were made using the pulse-echo technique with longitudinal sound pulses along the [111] direction. At 4 Mc/sec the attenuation was found to be 0.04 dB/cm independent of temperature in contrast with the results of Blitz *et al.* At $f < 10$ Mc/sec the attenuation is dominated by diffraction losses exhibiting a frequency dependence of $1/f$. At $f > 30$ Mc/sec the attenuation was found to be due to phonon-phonon losses with a frequency dependence of f^2 . Contribution to the attenuation from electron-phonon interactions was found to be negligible and independent of carrier concentration. By using the theory of sound absorption by Woodruff and Ehrenreich involving phonon-phonon interactions, an rms Grüneisen constant is deduced from the experimental data. This rms Grüneisen constant has a temperature dependence similar to the usual thermodynamic temperature-dependent Grüneisen constant.

I. INTRODUCTION

THE absorption of sound in germanium has been studied extensively.¹⁻¹⁰ At temperatures greater than 200°C and sound frequencies near 100 kc/sec, Kessler⁷ found that absorption is mainly due to lattice defects. At temperatures less than 300°K and frequencies greater than 1 Mc/sec, three mechanisms have been studied: sound absorption due to dislocations, electron-phonon interactions, and phonon-phonon interactions.

At room temperature Granato and Truell⁹ measured the ultrasonic attenuation between 12 and 300 Mc/sec. This they attributed to dislocations, although the correlation between the attenuation and dislocation density of their samples was poor. Lamb *et al.*² found no effect of dislocations on the sound adsorption in silicon for dislocation densities less than $10^4/\text{cm}^2$.

Electron-phonon interactions in *n*-type germanium have been suggested by Blitz *et al.*⁵ in order to explain a peak in the temperature dependence of the attenuation observed near 280°K. The experiment was performed at 4 and 6 Mc/sec using longitudinal sound pulses along the [111] crystallographic direction. Upon closer examination of electron-phonon interactions, as described by Weinreich,^{3,4} it appears that the relaxation

times of the electrons are much too short to allow any appreciable interaction at this temperature, thus resulting in negligible attenuation. At 4 and 6 Mc/sec the observed attenuation using the pulse technique is known to be almost entirely due to diffraction effects^{1,8,9}; any other attenuation is smaller by at least an order of magnitude. Since the attenuation due to diffraction is nearly temperature-independent, a temperature dependence resulting in a peak near 280°K would not be expected at 4 or 6 Mc/sec.

Dobbs *et al.*⁶ investigated the ultrasonic attenuation in germanium at 500 Mc/sec at temperatures less than 250°K. They credit the absorption to phonon-phonon interactions as described by Bömmel and Dransfeld.¹¹ The inaccuracies in their results were attributed to the problem of obtaining a good bond between the quartz transducers and the sample in certain temperature regions. Verma¹² fits the theory of Bömmel and Dransfeld to their data at temperatures less than 100°K by adjusting a temperature-independent Grüneisen constant so the theory will fit the data at 70°K. No attempt was made to compare the theory with the experimental data at higher temperatures. Since the Grüneisen constant in germanium has been shown to vary with temperature¹³⁻¹⁵ and the attenuation due to phonon-phonon interactions varies with the square of the Grüneisen constant, the assumption of a temperature-independent Grüneisen constant leads to appreciable error and must be modified.

With these problems in mind and because of the unexplained peak⁵ in the temperature dependence of the ultrasonic attenuation at 4 and 6 Mc/sec, it was decided to measure the ultrasonic attenuation in germanium over a wide frequency and temperature range in order to elucidate: (1) the extent and effect of diffraction and dispersion effects on ultrasonic attenuation measure-

* Supported by the U. S. Air Force Office of Scientific Research through Grant No. AFOSR-62-178.

† Raytheon Predoctoral Fellow.

¹ M. Redwood, Proc. Phys. Soc. (London) **B70**, 721 (1957).

² J. Lamb, M. Redwood, and Z. Shteinshliefer, Phys. Rev. Letters **3**, 28 (1959).

³ G. Weinreich, T. M. Sanders, Jr., and H. White, Phys. Rev. **114**, 33 (1959).

⁴ G. Weinreich, Phys. Rev. **107**, 317 (1957).

⁵ J. Blitz, D. M. Clunie, and C. A. Hogarth, in *Proceedings of the International Conference on Semiconductor Physics, Prague, 1960* (Czechoslovakian Academy of Sciences, Prague 1961, and Academic Press Inc., New York, 1961), p. 641.

⁶ E. Dobbs, B. B. Chick, and R. Truell, Phys. Rev. Letters **3**, 332 (1959).

⁷ J. O. Kessler, Phys. Rev. **106**, 646 (1957) and Phys. Rev. **106**, 654 (1957).

⁸ H. Seki, A. Granato, and R. Truell, J. Acoust. Soc. Am. **28**, 230 (1956).

⁹ A. Granato, and R. Truell, J. Appl. Phys. **27**, 1219 (1956).

¹⁰ W. P. Mason and T. B. Bateman, Phys. Rev. Letters **10**, 151 (1953).

¹¹ H. E. Bömmel and K. Dransfeld, Phys. Rev. **117**, 1245 (1960).

¹² G. S. Verma and S. K. Joshi, Phys. Rev. **121**, 396 (1961).

¹³ D. F. Gibbons, Phys. Rev. **112**, 136 (1958).

¹⁴ W. B. Daniels, Phys. Rev. Letters **8**, 3 (1962).

¹⁵ R. D. McCammon and G. K. White, Phys. Rev. Letters **10**, 234 (1963).

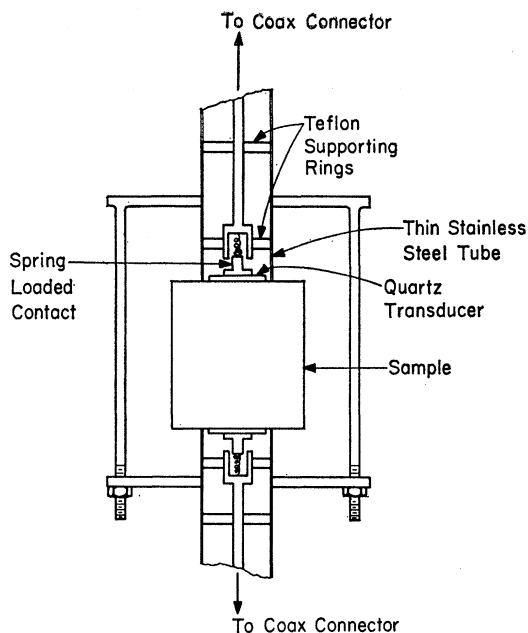


FIG. 1. Sample holder.

ments, (2) the magnitude of the contribution of electron-phonon interactions to the absorption of sound, and (3) the validity of the theory of sound absorption caused by phonon-phonon interactions as described by Bömmel and Dransfeld¹¹ and refined by Woodruff and Ehrenreich.¹⁶

II. EXPERIMENTAL RESULTS

The method used was the pulse-echo technique which consists of injecting a high-frequency sound pulse into a sample of germanium by means of a quartz transducer and measuring the amplitudes of the successive internally reflected echoes. The attenuation α is determined by fitting an exponential to the decay pattern of the received echoes. The experiment was performed between 20 and 350°K with longitudinal sound waves of frequencies ranging from 4 to 132 Mc/sec traveling along the [111] crystallographic axis.

Figure 1 shows a sketch of the sample holder. The sample is supported by thin-walled stainless steel tubing which touch the parallel faces of the sample. This method of support results in negligible sound absorption at the end faces and affords good electrical contact at all temperatures.

Sound pulses of about 3- μ sec duration were used. The transducers were X-cut quartz disks cut to resonate at the injection frequency or one of its odd subharmonics. The echoes were received by the transmitting transducer (single-ended system) or by a second transducer on the opposite face of the sample (double-ended system). The latter mode of operation was preferred

¹⁶ T. O. Woodruff and H. Ehrenreich, Phys. Rev. **123**, 1553 (1961).

TABLE I. Sample data.

	Resistivity	Dislocation density	Length	Average diameter
Sample 1	40 Ω -cm	4000/cm ²	3 cm	2.5 cm
Sample 2	0.0009 ^a Ω -cm	7500/cm ²	2 cm	2 cm

^a Arsenic doped *n*-type germanium.

because it provides isolation between input and output circuits. The received echoes were amplified and displayed unrectified on an oscilloscope as shown in Fig. 2. The displayed echoes were either measured directly by means of a variable attenuator so as to keep the gain of the system constant, or they were photographed and measured. By using a receiving system with constant gain and leaving the echoes unrectified it was possible to keep nonlinearities of the detection system at a minimum. This kept the error in the measurement of the attenuation from this source to within 2% at frequencies below 60 Mc/sec. At the higher frequencies the use of a crystal mixer increased these errors to about 5%.

The properties of the two germanium samples used in this work are listed in Table I. The shape of the samples was approximately cylindrical. The top and bottom surfaces were ground and lapped flat and parallel to within 3×10^{-5} cm. This is necessary in order to minimize errors in the measurement of the attenuation. When the end surfaces of the sample are not parallel, then upon each reflection of the longitudinal sound pulse at these ends, some of the energy will be directed toward the sample walls, while some will be lost by conversion to a transverse mode. The longitudinal sound energy that hits the side walls will in part be lost by conversion to a transverse mode. Another part will be reflected as a longitudinal mode and is then able to interfere with the main longitudinal sound pulse. These losses caused by mode conversion and interference effects result in an overestimate of the attenuation. By using surfaces flat to less than 3×10^{-5} cm instead of 3×10^{-3} cm a decrease in attenuation by as much as a factor of 3 was observed. The attenuation due to the bond is caused by sound absorption and mode conversion in the bond. The bond absorption can be estimated and corrected for by using a substitution

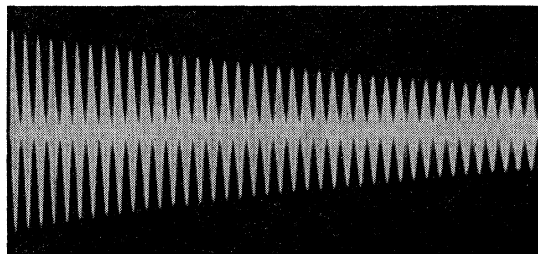


FIG. 2. Typical display of the unrectified echoes. Frequency = 12 Mc/sec, $T = 300^\circ\text{K}$. The above display shows echoes number 20 to 50. In this case 525 echoes were measured.

technique as described by Redwood.¹⁷ Using this method we found our bond losses to be 0.008 ± 0.003 dB per reflection at 300°K . This loss was found to vary only slightly with temperature, in agreement with the results of Hunters *et al.*¹⁸ in Dow Corning 200. The bonding layer thickness was about 5×10^{-5} cm. The thickness was measured by using a Sheffield gauge. The height of the transducer resting on the sample without the bonding layer was measured and subtracted from the total height of the transducer-bonding layer-sample stack.

The bonding agents used were Nonaq,¹⁹ which gave satisfactory bonds between 220 and 400°K and Dow Corning 200 silicone oils²⁰ of various viscosities.²¹ These oils bond well from 300°K to the lowest temperatures. The quality of the bond is determined by the similarity of the envelopes of the echoes to the input pulse. Within experimental error there was no difference in the attenuation within the overlapping temperature ranges of different bonding materials.

Diffraction Effects

The sound wave is not a plane wave as it leaves the quartz transducer but a diverging wave. This follows from considering a piston source whose diameter is not too much larger than the wavelength λ of the sound. The intensity of a piston source is given by

$$I = I_0 \left\{ \frac{2J_1[(2\pi a/\lambda) \sin\theta]}{(2\pi a/\lambda) \sin\theta} \right\}^2, \quad (1)$$

where a = piston radius, J_1 the first-order cylindrical Bessel function, and θ the angle with respect to the piston axis. The angular spread of the first sound lobe obtained from Eq. (1) with $\lambda \ll a$ is

$$2\theta = 1.2\lambda/a. \quad (2)$$

For $a = 0.95$ cm^{21a} this gives $2\theta = 10^\circ$ at 4 Mc/sec and $2\theta = 0.8^\circ$ at 60 Mc/sec. Hence the wave is far from being plane at 4 Mc/sec. This spreading beam experiences

¹⁷ M. Redwood (Ref. 1). This method consists of putting a transducer on face A , keeping the opposite face (face C) free and measuring the attenuation α_A . Then without disturbing face A , one puts a transducer on face C . The attenuation α_{CA} is measured by using this transducer for both sending and receiving. Then without disturbing face C one removes the transducer from face A , making sure face A is clean. α_C is then measured using transducer C only. The attenuation due to the bonding layer on face A is

$$\alpha_{\text{corr}} = \alpha_{CA} - \alpha_C,$$

and the true attenuation as measured from face A is

$$\alpha_{\text{true}} = \alpha_A - \alpha_{\text{corr}}.$$

¹⁸ J. L. Hunter, T. B. Lewis, and C. J. Montrose, *J. Acoust. Soc. Am.* **35**, 481 (1963).

¹⁹ Nonaq Stopcock grease, distributed by Fisher Scientific Company, Chicago, Illinois.

²⁰ Dow Corning Silicone Oils. Dow Corning Corp., Midland, Michigan.

²¹ Viscosities used were 3, 800, 10 000, and 2.5×10^6 centistokes.

^{21a} Note added in proof.

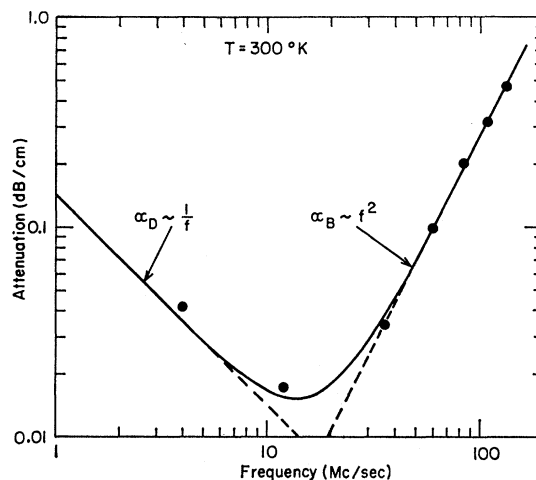


FIG. 3. Comparison of the theoretical and experimental frequency dependence of the attenuation at room temperature. Line α_D , the theoretical diffraction loss, is estimated using our sample geometry. Line α_B is the f^2 dependence expected from phonon-phonon losses. This line has been adjusted to match the experimental results at 60 Mc/sec. The solid curve is $\alpha_B + \alpha_D$ and gives the expected frequency dependence of the total attenuation. The solid circles represent the present experimental results using sample 1.

reflection and mode conversion at the side wall of the sample. Mode conversion drains energy from the initial wave. Redwood calculated this loss for germanium assuming the transducer radius to be equal to the sample radius and found that this loss is proportional to θ . By extending his calculation to cases where the sample radius is larger than the transducer radius one obtains for our geometry the attenuation arising from this diffraction effect, α_D , which is shown as in Fig. 3. Because of Eq. (2), α_D varies with the sound frequency as $\alpha_D \propto f^{-1}$. It varies with temperature by only about 1% over the whole temperature range through its dependence on the sound velocity.²² Hence we consider α_D to be temperature-independent.

Upon hitting the side walls, part of the sound wave will be reflected in its original mode and give rise to interference effects. These result in an oscillatory variation of the echo amplitudes as a function of echo number. Redwood, again assuming equal transducer and sample radii, found that one should observe minima in these oscillations at $\lambda d/A = 1.7\pi, 5\pi, 8\pi \dots$, and maxima at $\lambda d/A = 3.5\pi, 6\pi, 10\pi \dots$, where d is the distance of sound travel and A the transducer area. For our geometry this corresponds to minima at echo numbers 30, 89, 142 \dots and maxima at echo numbers 61, 105 \dots as shown in Fig. 4.

The attenuation is measured by plotting the logarithm of the echo amplitude versus the echo number and then by drawing a straight line through the nodal

²² Redwood (Ref. 1) shows that α_D varies as the square of the velocity. The velocity varies less than 0.5% over the temperature range of interest. See H. J. McSkimin, *J. Appl. Phys.* **24**, 988 (1953).

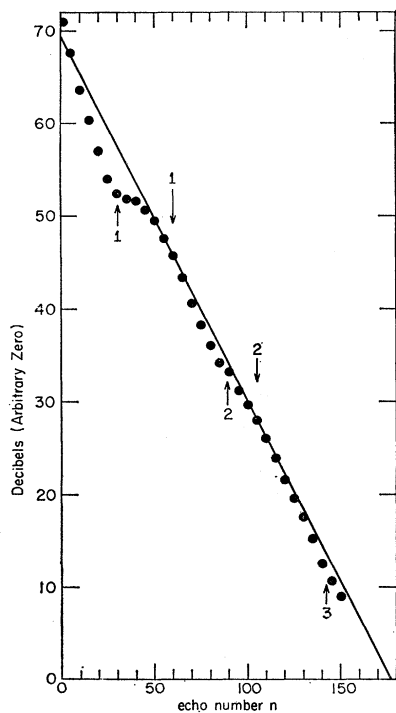


FIG. 4. Typical plot of the logarithm of the amplitudes of the echoes in dB as a function of echo number. The upward pointing arrows are where the predicted 1st, 2nd, and 3rd troughs should occur and the downward pointing arrows are where the predicted 1st and 2nd peaks should occur. The slope of the straight line through the peaks gives the attenuation.

points of the resulting oscillations. The slope of this line is then the attenuation. In some cases it was found more convenient to draw the straight line through the peaks of the oscillations as shown in Fig. 4. The difference in the attenuation between using nodal points and peaks is within 1%. The error in the measurement of the attenuation by either method can be as large as 5%, depending on whether a sufficient number of echoes are observed. The larger errors occur when there are insufficient echoes to cause more than one oscillation. This, however, is a systematic error and does not affect the accuracy of the temperature dependence of the attenuation. It should be noted that deviations from parallelness of the top and bottom surfaces give rise to effects which are very similar to those due to diffraction.

The total absolute error at 300°K is between 5 and 10% depending on the frequency used; this error consists of uncertainties in the correction for bond losses, in the amplitude determination due to receiver nonlinearities, and in the graphic determination of the attenuation. Since the temperature dependence of the attenuation is of concern, a more realistic error is the error in the attenuation with respect to the 300°K value of attenuation. This error is less than 5%.

III. RESULTS

Figure 2 shows a typical photograph of the received echoes numbering in this case from 20 to 50. More than 400 echoes could often be observed. The attenuation measured with sample 1 at 300°K is plotted as a function of frequency and compared with theory in Fig. 3. After correcting for the bond losses the attenuation α

can be represented as the sum of two terms

$$\alpha = \alpha_B + \alpha_D, \quad (3)$$

where α_B is the bulk attenuation and α_D the attenuation due to diffraction effects which cause mode conversion at the walls of the sample. The quantitative agreement between the experimental data below about 10 Mc/sec and α_D calculated from Redwood's theory shows that diffraction losses dominate the attenuation at the lower frequencies. Figure 4 shows a plot of the logarithm of the echo amplitudes versus echo number. The oscillatory change of the amplitudes is clearly visible and it is seen that the positions of the maxima and minima agree well with the predictions of the interference calculation.

The attenuation measured at 4 Mc/sec is shown as a function of temperature in Fig. 5. The attenuation is very nearly temperature-independent as expected from the theory of diffraction losses. This is taken as an additional confirmation for the fact that α_D dominates the attenuation at these lower frequencies. Figure 5 shows also the results of Blitz *et al.*⁵ obtained at the same frequency. Their attenuation is larger than ours by almost two orders of magnitude. This difference in attenuation might be caused by their use of a small diameter transducer, since the defraction loss varies as the reciprocal of the transducer area. However this does not explain their attenuation peak near 280°K, which is surprising since both experiments were performed using almost identical samples and the same sound mode and propagation direction.

As seen from Fig. 3, diffraction losses have a negligible effect on the attenuation at frequencies above 30 Mc/sec. At these higher frequencies the attenuation is proportional to f^2 which is the expected frequency dependence at 300°K if phonon-phonon interactions dominate the loss mechanism. Figure 6 shows the temperature dependence of the attenuation at 60 Mc/sec for

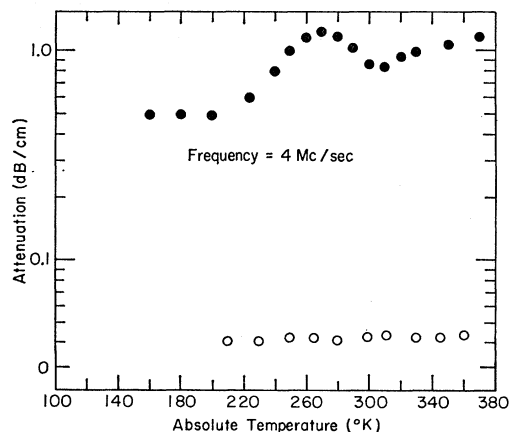


FIG. 5. Ultrasonic attenuation as a function of temperature at 4 Mc/sec. ● Blitz's results in 11- Ω -cm phosphorus-doped *n*-type germanium; ○ results using sample 1.

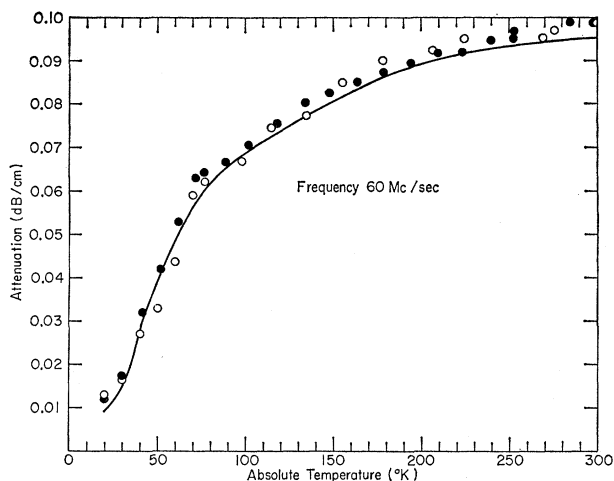


FIG. 6. Ultrasonic attenuation as a function of temperature at 60 Mc/sec. ● sample 1; ○ sample 2. The solid line gives α_{pp} after correcting the data of sample 1 for bonding and electron-phonon losses.

the pure and the degenerate n -type germanium sample. In spite of the difference of the carrier concentration between the two samples no difference was found in their attenuation between 20 and 300°K. The attenuation of sample 1 was also measured as a function of temperature at 132 Mc/sec.

IV. DISCUSSION

The qualitative agreement between the measured attenuation below 10 Mc/sec and the theory of diffraction effects shows clearly that the attenuation is dominated by diffraction losses at the lower frequencies. At the higher frequencies the attenuation is proportional to f^2 which suggests that phonon-phonon interactions are the source of the loss mechanism. Loss mechanisms caused by lattice defects, dislocations, and electron-phonon interactions give rise to attenuation values much smaller than those measured in the present temperature and frequency ranges. From the work of Kessler⁷ we estimate the attenuation caused by lattice defects to be 10^{-14} dB/cm for 1 Mc/sec and 10^{-16} dB/cm for 100 Mc/sec at 300°K. According to the model of Granato and Truell⁹ the contribution to the attenuation from dislocation densities $\leq 10^4$ per cm^2 is 10^{-4} dB/cm or less at 100 Mc/sec. This is much less than our measured attenuation.

The losses arising from electron-phonon interactions can be estimated from the theory of Weinreich.^{3,4} These losses were found to be negligible except in the 20 to 60°K temperature region where they are less than 2% of the measured attenuation. For frequencies less than 200 Mc/sec the expression for the attenuation as given by Weinreich can be shown to be

$$\alpha_{ep} = C(n\tau\omega^2/T), \quad (4)$$

where α_{ep} = attenuation due to electron-phonon inter-

action, n = carrier concentration, τ = intervalley relaxation time, ω = angular frequency of the sound wave, T = temperature, and C = a constant dependent on the direction and, polarization of the sound wave. For carrier concentrations less than $10^{17}/\text{cc}$ and temperatures from 20 to 60°K Weinreich found the product $n\tau$ to be independent of n . In this range the attenuation, α_{ep} , should be independent of impurity concentration. At lower temperatures the attenuation will become negligible since the number of carriers decreases exponentially. At the higher temperatures α_{ep} will also become negligible due to the exponential dependence of τ on T and the $1/T$ term in Eq. (4). In order to extract the attenuation due to phonon-phonon interaction, α_{ep} must be subtracted from α_B .²³ The solid line in Fig. 6 shows the attenuation due to phonon-phonon interactions, after correcting the data for bond and electron-phonon losses. For carrier concentrations in excess of $10^{18}/\text{cc}$ (degenerate germanium) $n\tau$ is independent of temperature and Eq. (4) shows that in this case at low temperatures, α_{ep} will get very large. At higher frequencies and lower temperatures, Mason and Bateman¹⁰ have observed the temperature dependence predicted by Eq. (4) in degenerate germanium. However, at $T > 20^\circ\text{K}$ the product $n\tau$ is such that α_{ep} is about the same as in the nondegenerate case. This explains why there is no difference in the observed attenuation between the pure and the degenerate sample (see Fig. 6).

Phonon-Phonon Losses

There are two types of phonon-phonon interactions which cause attenuation. One is a thermoelastic loss as described by Zener.²⁴ This is caused by the flow of heat from a region of compression to a region of rarefaction due to the sound wave in the material. In germanium at room temperature this loss is about 10^{-5} dB/cm at 60 Mc/sec and 7×10^{-5} dB/cm at 132 Mc/sec. This loss is two orders of magnitude below the measured attenuation and can be neglected.

The other process which qualitatively accounts for the temperature dependence and the magnitude of the observed attenuation is due to a mechanism proposed by Akhieser²⁵ and expanded by Bömmel and Dransfeld¹¹ and Woodruff and Ehrenreich.¹⁶ In this process the sound wave modulates the elastic properties and hence the phonon frequencies of the medium through which it propagates. These modulated phonons are no longer in thermal equilibrium but tend to relax toward thermal equilibrium via phonon-phonon collisions caused by anharmonic interactions. This relaxation produces

²³ By using Eq. (3) for longitudinal sound waves at 60 Mc/sec along the [111] direction, this contribution was estimated to be 0.0005 dB/cm at 40°K about 2% of the total attenuation. In this manner α_{ep} was always found to be less than 2% of the total attenuation.

²⁴ C. Zener, *Elasticity and Anelasticity in Metals* (The University of Chicago Press, Chicago, 1948), p. 89.

²⁵ A. Akhieser, *J. Phys. (U.S.S.R.)* 1, 277 (1939).

entropy and hence removes energy from the sound wave.

Woodruff and Ehrenreich¹⁶ arrive at their equation (4.10) by making the following assumptions:

(i) The material is an isotropic Debye solid, having a constant average velocity of sound v_D , defined by

$$(3/v_D^3) = (1/v_l^3) + (2/v_t^3), \quad (5)$$

where v_l and v_t are the longitudinal and transverse sound velocities, respectively. A consequence of this is that

$$\omega_{qb} = v_D |\mathbf{q}|, \quad (6)$$

where ω_{qb} is the frequency of the phonon in branch b and of wave number \mathbf{q} .

(ii) The normal and umklapp relaxation times are independent of the direction of \mathbf{q} . They are dependent on $|\mathbf{q}|$ and b .

(iii) The umklapp processes dominate in the relaxation of the phonons. This relaxation time τ is defined as

$$\kappa \equiv \frac{1}{3} C_v V_D^2 \tau, \quad (7)$$

where C_v is the specific heat, and κ the thermal conductivity.

(iv) $\omega\tau \ll 1$.

These assumptions limit the theory to a qualitative explanation of the attenuation, α_{pp} , resulting from phonon-phonon interactions. Because of the qualitative nature of the theory a further assumption is made, namely that the local temperature inside the crystal is equal to the external temperature. This gives the relation.

$$\alpha_{pp}(T) = \frac{8.68 \langle \gamma^2 \rangle_{av} \omega^2 T \kappa \tan^{-1}(2\omega\tau)}{\rho v_D^5 (2\omega\tau)} \text{ in dB/cm}, \quad (8)$$

where ρ = density of germanium and $\langle \gamma^2 \rangle_{av}$ = the average of the square of the Grüneisen constant defined by,

$$\langle \gamma^2 \rangle_{av} = \frac{\sum_{qb} \gamma_{qb}^2 C_{qb}}{\sum_{qb} C_{qb}} \quad (9)$$

and

$$C_{qb} = k \left(\frac{\hbar \omega_{qb}}{kT} \right)^2 \frac{\exp \frac{\hbar \omega_{qb}}{kT}}{\left(\exp \frac{\hbar \omega_{qb}}{kT} - 1 \right)} \quad (10)$$

and

$$\gamma_{qb} = - \frac{d[\ln \omega_{qb}]}{d[\ln V]}, \quad (11)$$

where V = volume, and k = Boltzmann's constant.

At high temperatures Eq. (8) reduces to $\alpha_{pp} \propto \omega^2$ in agreement with the experimental results. Using values

of thermal conductivity given by Slack and Glassbrenner,²⁶ heat capacity given by Flubacher *et al.*,²⁷ and the Grüneisen constant from Gibbons,¹³ the attenuation was computed for 60 Mc/sec at 300°K using Eq. (8). α_{pp} was found to be 0.23 dB/cm. This value should be compared with the experimental value $\alpha_{pp} = 0.095$ dB/cm. The discrepancy shows the qualitative nature of the theory. It is not evident why the theory should yield an overestimate of α_{pp} . In order to compare the temperature dependence of the attenuation with the theory, the experimental and theoretical values of $\alpha_{pp}(T)/\alpha_{pp}(300^\circ\text{K})$ are plotted as a function of temperature in Fig. 7. The theoretical curve A in Fig. 7 is based on a temperature-independent Grüneisen constant. This procedure was used by Verma *et al.*¹² and others,^{11,16} and in this case yields a strong peak in α_{pp} near 50°K in disagreement with the experimental results. By taking the temperature dependence of the thermodynamic Grüneisen constant $\langle \gamma \rangle_{av}$ as measured by McCammon, curve B in Fig. 7 was obtained. This gives a much better fit and shows the errors involved in assuming a Grüneisen constant independent of temperature. However, the thermodynamic Grüneisen

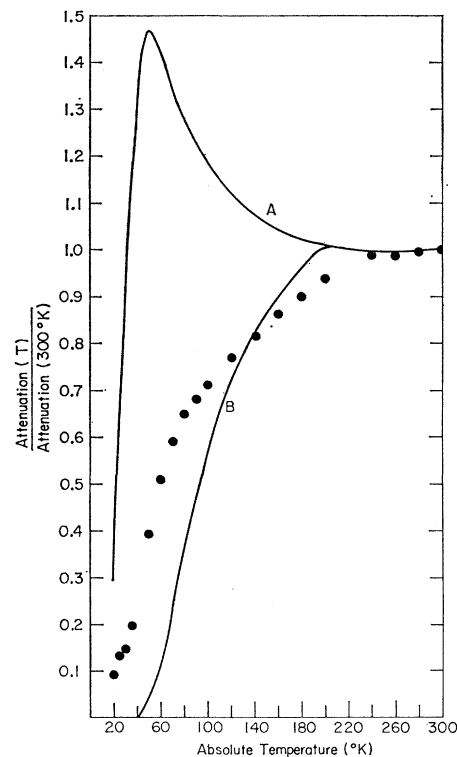


FIG. 7. Plot of $\alpha_{pp}(T)/\alpha_{pp}(300^\circ\text{K})$ at 60 Mc/sec. The points are the corrected results taken from Fig. 6. Line A is the theoretical curve obtained using a Grüneisen constant independent of temperature. Line B is the theoretical curve using the thermodynamic temperature-dependent Grüneisen constant as given by McCammon (see text).

²⁶ G. A. Slack and C. Glassbrenner, Phys. Rev. 120, 782 (1960).

²⁷ P. Flubacker, A. J. Leadbetter, and J. A. Morrison, Phil. Mag. 4, 273 (1959).

constant is defined as

$$\langle \gamma \rangle_{av} = \sum_{qb} \gamma_{qb} C_{qb} / \sum_{qb} C_{qb}, \quad (12)$$

hence curve B in Fig. 7 is derived by substituting $\langle \gamma \rangle_{av}^2$ for $\langle \gamma^2 \rangle_{av}$ in Eq. (8). This results in a different temperature dependence of $\alpha_{pp}(T)/\alpha_{pp}(300)$ than if $\langle \gamma^2 \rangle_{av}$ were used. The temperature dependence of $\langle \gamma^2 \rangle_{av}$ is unfortunately not known and the predictions of the theory of Woodruff and Ehrenreich can therefore not be further tested. If one assumes, however that the theory correctly describes the temperature dependence of the attenuation, then $\langle \gamma^2 \rangle_{av}$ can be obtained as a function of temperature from the experimental results and Eq. (8). This equation is based on the assumption that $\omega\tau < 1$, which implies for our case at 60 Mc/sec the condition $T \geq 30^\circ\text{K}$. Upon closer examination of the theory of Woodruff and Ehrenreich it appears, however, that a good qualitative determination of $\langle \gamma^2 \rangle_{av}$ can be obtained at lower temperatures.

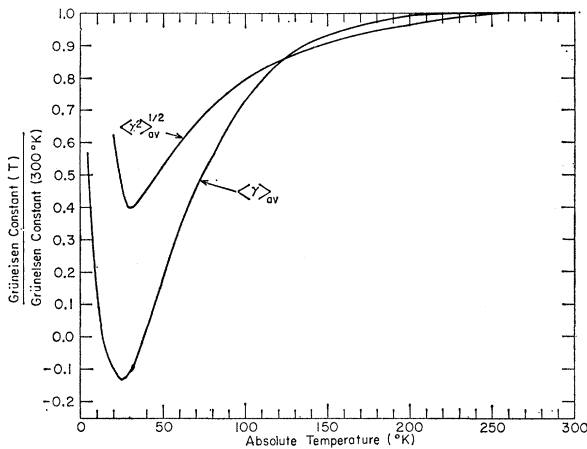


FIG. 8. Plot of $\langle \gamma^2 \rangle_{av}^{1/2}$ and $\langle \gamma \rangle_{av}$ as a function of temperature both quantities normalized to their respective values at 300°K .

Figure 8 shows a plot of $\langle \gamma \rangle_{av}$ and $\langle \gamma^2 \rangle_{av}^{1/2}$, the rms Grüneisen constant, versus temperature, both quantities normalized to their respective values at 300°K . In both cases there is a minimum in these quantities near 30°K followed by a sharp rise as the temperature is decreased further.²⁸ The temperature dependence of $\langle \gamma^2 \rangle_{av}^{1/2}$ as obtained from the experimental results and Eq. (8) is less than that of $\langle \gamma \rangle_{av}$. This is to be expected since negative signs of some of the γ_{qb} can even lead to negative values of $\langle \gamma \rangle_{av}$ whereas $\langle \gamma^2 \rangle_{av}^{1/2}$ is always positive.

The validity of the temperature dependence as a

²⁸ Dr. E. R. Dobbs pointed out to me that he had also determined the rms Grüneisen constant from his earlier work (see Ref. 6) on ultrasonic attenuation in germanium [E. R. Dobbs, in *The Seventh International Conference on Low Temperature Physics, Toronto, 1960* (University of Toronto Press, Toronto, 1960), p. 291]. He referred to it as the acoustic Grüneisen constant. Above 40°K his rms Grüneisen constant agrees well with ours also showing a rise below 40°K ; however, he incorrectly extrapolated the rms Grüneisen constant to zero at zero temperature.

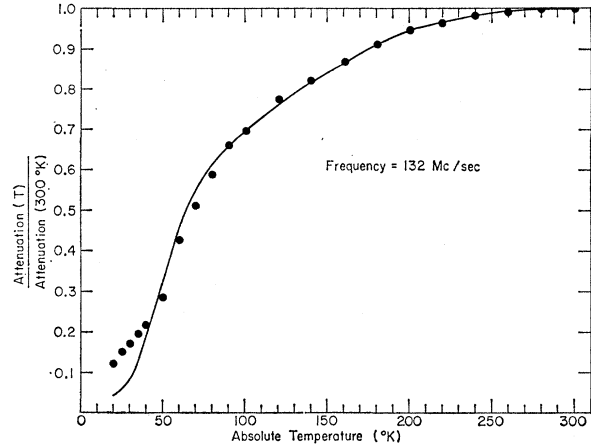


FIG. 9. Plot of $\alpha_{pp}(T)/\alpha_{pp}(300^\circ\text{K})$ at 132 Mc/sec. The solid line represents the theoretical curve using the rms Grüneisen constant from Fig. 8. The points represent the data corrected for bonding and electronphonon losses.

function of frequency of Eq. (8) can be checked by calculating $\alpha_{pp}(T)/\alpha_{pp}(300)$ at 132 Mc/sec from Eq. (8) using $\langle \gamma^2 \rangle_{av}$ as determined above at 60 Mc/sec. This was done and Fig. 9 shows the comparison between theory and experiment at 132 Mc/sec. Above 40°K the comparison is good, getting worse at the lower temperatures. This is probably due to the fact that at 132 Mc/sec $\omega\tau \geq 1$ for temperatures less than 40°K and the theory as given by Eq. (8) starts to break down resulting in this low-temperature deviation.

V. CONCLUSION

The ultrasonic attenuation of megacycle sound waves in germanium appears to be dominated by diffraction effects at the lower frequencies and by phonon-phonon interactions at the higher frequencies. At lower temperatures electron-phonon interactions may contribute to the attenuation, but only slightly. Only in degenerate germanium may this contribution become quite large at higher frequencies and lower temperatures. Any attenuation due to dislocations appear to be negligible for samples with dislocation densities less than $10^4/\text{cm}^2$. We were unable to reproduce the high attenuation and the attenuation peak near 280°K observed by Blitz *et al.* The phonon-phonon theory of Woodruff and Ehrenreich can be used to get a rms value for the Grüneisen constant which shows a temperature dependence similar to that of the usual thermodynamic Grüneisen constant. The use of this rms Grüneisen constant in the phonon-phonon theory of sound absorption gives good agreement between theory and experiment for the temperature dependence as a function of frequency, when $\omega\tau < 1$.

ACKNOWLEDGMENTS

The author would like to thank Dr. H. Fritzsche for his helpful suggestions and encouragement through all phases of this work.

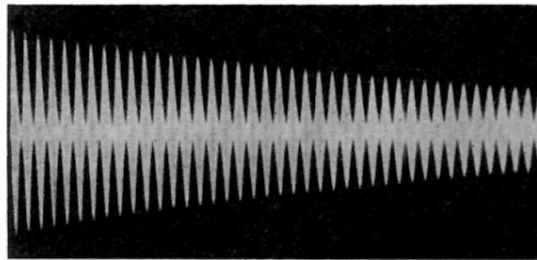


FIG. 2. Typical display of the unrectified echoes. Frequency = 12 Mc/sec, $T = 300^\circ\text{K}$. The above display shows echoes number 20 to 50. In this case 525 echoes were measured.